

Article

# Performance Evaluation of Control Compatibility for an OTEC Pump Shutdown Condition

Seungtaek Lim <sup>\*</sup> , Jiwon Yoon, Hosaeng Lee and Hyeonju Kim 

Seawater Energy Plant Research Center, Korea Research Institute of Ships & Ocean Engineering,  
Daejeon 34103, Republic of Korea

\* Correspondence: limst@kriso.re.kr; Tel.: +82-33-630-5023

**Abstract:** South Korea is currently in the preparatory stage of commercializing an ocean thermal energy conversion (OTEC) system, as the demonstration of a 1 MW scale OTEC system has been accomplished. However, the commercialization of OTEC requires the establishment of a control system for various environmental changes. Therefore, pre-emptive identification of the system's risk factors and the process of analyzing the impact of the system, building control items, and optimizing control are necessary. This study aims to establish and analyze an optimized control system for MW-scale OTEC risk factors, such as the shutdown of seawater or refrigerant pumps. The selected OTEC system was designed for 1070 kW class facilities, with a 36.6% portion of total electricity usage by the seawater pump and refrigerant pump. As a result, an on/off control system was adopted in order to eliminate the risk factors. By adjusting this option, dry operation of the refrigerant pump, water hammering, and liquid inflow into the turbine were successfully prevented. To be more specific, the initial system was to be shut down due to a sharp decrease in power at the point where the deep seawater flow rate was 538 kg/s (35.7% of max flow rate) and the surface seawater flow rate was 715 kg/s (38.4% of max flow rate). This situation was improved by adopting parallel operation of seawater pumps and on/off control, thereby leading to a more stabilized operation by maintaining a flow rate of over 1864 kg/s for surface seawater and 1507 kg/s for deep seawater. Moreover, it was confirmed that the flow rate of the pump was reduced by 1.89 kg/s per second in the process of pump shutdown during a single operation mode of the refrigerant pump. Parallel operation made it possible to maintain 60.2% of the output by increasing the power of the second pump's flow rate in the event of the first pump shutting down. The final seawater temperature differential power generation model derived from this study consists of two refrigerant pumps and two surface seawater and deep seawater pumps in order to prevent system shutdown caused by a single pump failure. The final design was reflected in the final delivery to Kiribati, which is located near the equator.

**Keywords:** closed cycle; control logic; hazard analysis; ocean thermal energy conversion (OTEC); shut down



**Citation:** Lim, S.; Yoon, J.; Lee, H.; Kim, H. Performance Evaluation of Control Compatibility for an OTEC Pump Shutdown Condition. *J. Mar. Sci. Eng.* **2023**, *11*, 155. <https://doi.org/10.3390/jmse11010155>

Academic Editors: Rafael Morales, Eva Segura and Yassine Amirat

Received: 13 October 2022

Revised: 23 November 2022

Accepted: 15 December 2022

Published: 9 January 2023



**Copyright:** © 2023 by the authors. Licensee MDPI, Basel, Switzerland. This article is an open access article distributed under the terms and conditions of the Creative Commons Attribution (CC BY) license (<https://creativecommons.org/licenses/by/4.0/>).

## 1. Introduction

Humanity is in the process of developing alternative energy sources in order to cope with increased energy consumption and the depletion of fossil fuel resources. In addition, the development of renewable energy is accelerating for the prevention of global environmental pollution [1]. Renewable energy consumption is expected to rise from 17.4 billion Btu in 2012 to 25.1 billion Btu by 2040, accounting for 44.2% of the world's industrial energy consumption [2].

Ocean thermal energy conversion (OTEC) technology is a method for generating electricity using the temperature difference between relatively warm surface seawater (annual average temperature of 25~30 °C) and deep seawater (annual average temperature of 2~5 °C). This technology is characterized by a semi-infinite resource (seawater) and

high operation rate throughout the year due to the small seasonal temperature changes in seawater [3].

OTEC types differ in terms of the working fluid used in their cycle. The open cycle uses surface seawater itself as the working fluid. Various research studies are currently being conducted to address the emerging global water shortage problem [4]. Fresh water, a byproduct of the open-cycle OTEC, can contribute to solving this problem and also produce renewable energy.

The closed cycle, the most common method used in OTEC, uses low-temperature refrigerants as the working fluid. Closed-type OTEC pilots and demonstration plants are now being actively constructed in Japan, Europe, and other countries, following the construction of a 50 kW plant in the United States in 1979.

South Korea was the fourth country to construct a 20 kW pilot-scale plant in 2013 and is currently constructing a demonstration plant of 1 MW in Kiribati, which is a South Pacific island country [5–8]. In South Tarawa, Kiribati, the annual temperature of the sea surface seawater is 28–30 °C, and that of the deep seawater at a depth of 1000 m is 5 °C, which would make OTEC plants located in South Tarawa particularly efficient and able to produce power 24/7 and year-round [9]. Figure 1 shows the domestic demonstration of a floating OTEC plant in South Korea.



**Figure 1.** Demonstration of 1 MW floating OTEC in Republic of Korea.

Recent studies of OTEC systems have focused on the stabilization and control of system operations. In Japan, studies adopting PI control to reduce the time taken to achieve the desired output, as well as developing a control system for the OTEC cycle's flow rate, are underway [10,11]. In advance of studies on the control optimization of such a system, a control module that can deal with environmental changes or risk factors that occur in a particular situation is necessary. Industries are widely using risk assessment and hazard analyses in order to derive solutions for the occurrence of such hazards in plants or facilities [12,13]. In addition, such assessments have been used to predict system impacts through risk analysis based on the scenario of a pump shutting down at a nuclear fuel facility. The effects of risk factors such as pipe ruptures and pump failures on a large water pipe supply system were analyzed [14,15]. Such risk factor analysis is applied in many technical fields. In preliminary hazard list (PHL) analysis, risk factor analysis and the effects on devices are classified for detailed risk analysis. The composition of an OTEC system consists of structures, power generation facilities, water intake facilities, and risers. Risk factors include natural factors such as earthquakes and changes in seawater temperature; human factors such as abnormal operation; and factors that occur during operation, including long-term operation. The effects of risk factors range from extreme situations, in which plant destruction occurs, to high-risk situations, in which system shutdown occurs, to low-risk situations, in which system efficiency is reduced.

In this study, among the various risk factors affecting OTEC, as listed in Table 1, conditions in which seawater and refrigerant pumps shut down, causing a system to halt

operation, were simulated, and the expected risk factors were analyzed. In addition, flow rate stabilization was confirmed through parallel control, and an improved process model was presented. In addition, control system data are to be adjusted for an OTEC plant demonstration in the near future.

**Table 1.** Results of the MW-scale OTEC Preliminary Hazard List analysis.

Preliminary Hazard List Analysis			
No.	System Item	Hazard	Hazard Effects
1	Buoyant Structures	-Unbalanced buoyancy -Damage by external force -Change in marine environment -Weather phenomena	-Sinking -Loss of buoyancy -Instability
2	Mooring System	-Damage by external force -Long-term exposure to seawater -Maintenance of deep seawater connection parts -Vulnerable parts	-Fracture -Loss of structure -Instability -Corrosion -Defects
3	Foundation Structures	-Insufficient data on deep seawater -Ground fluctuation (e.g., earthquake) -Damage by external force	-Fracture, defects -Structural fluctuation
4	Riser System	-Vibration caused by long-term exposure to marine environment -Damage by external force -Abnormal operation -Fracture of junction with floating structure	-Fracture -Structural fluctuation -Overflow of mooring, buoyancy, and riser systems -Generation efficiency decline
5	Generation Facilities	-Electric converting disability -Damage by external force	-Generation efficiency decline -Refrigerant leakage -Refrigerant Pump shutdown
6	Seawater Intake Facility	-Unstable electric supply -Inflow of particles -Damage by external force	-Pump shutdown -Pump efficiency decline -Seawater leakage

## 2. OTEC System Performance Analysis

### 2.1. Closed-Cycle OTEC System

#### 2.1.1. Cycle Physical Theory of the OTEC System

The closed-type OTEC (CC-OTEC) uses the temperature difference between surface seawater and deep seawater to allow the working fluid to pass through the turbine and generate heat energy, which is converted into electricity.

The increase in cycle efficiency is proportional to the temperature difference between surface water and deep seawater. In the case of surface seawater, the temperature varies from 25~31 °C, depending on seasonal and regional situations. Deep seawater, with a depth of more than 1000 m, shows an annual temperature around 5 °C, regardless of region and season [16].

The working fluid, which is liquefied in the condenser, is stored in the refrigerant tank. Equations (1) and (2) show the total heat transfer rate of evaporation and condensation. Equation (3) is the output for CC-OTEC’s turbine, and Equation (4) presents the net power:

$$Q_e = m_{sw} C_p (T_{sw.in} - T_{sw.out}) \tag{1}$$

$$Q_c = m_{dw} C_p (T_{dw.out} - T_{dw.in}) \tag{2}$$

$$W_{tb} = m_r \eta_{tb} (h_{tb.in} - h_{tb.out}) \tag{3}$$

$$W_{net} = W_{tb} - W_{dwp} - W_{swp} - W_{rp} \tag{4}$$

where  $m_r$  is the mass flow rate of the refrigerant;  $m_{ww}$  and  $m_{cw}$  are the mass flow rate of the surface seawater and deep seawater;  $c_p$  is the specific heat at constant pressure;  $\eta_{tb}$  is the turbine efficiency;  $T_{ww}$  and  $T_{cw}$  are the temperatures of deep seawater and surface seawater, respectively; and  $h_{tb}$  is the enthalpy of the turbine. In this system, the refrigerant that passes through the evaporator completely evaporates and enters the turbine in the form of dry steam. For this energy calculation, reference was made to the existing literature to derive the power consumption and generation output of the OTEC system [17]. Figure 2 shows the schematic diagram of the MW-scale CC-OTEC.

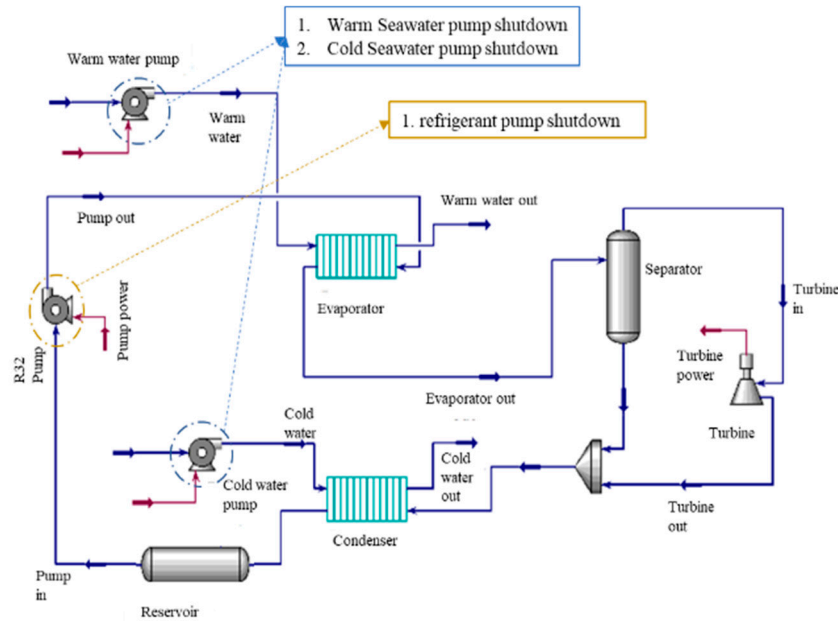


Figure 2. Closed-cycle OTEC.

In this case, net efficiency is calculated as in Equation (5), and the output of the refrigerant pump, surface seawater, and deep seawater is shown in Equations (6)–(8), respectively:

$$\eta_{net} = (W_{tb} - W_{dwp} - W_{swp} - W_{rp}) / Q_e \tag{5}$$

$$W_{rp} = m_r \eta_{rp} (h_{rp,in} - h_{rp,out}) \tag{6}$$

$$W_{dwp} = m_{dw} \eta_{dwp} (h_{dwp,in} - h_{dwp,out}) \tag{7}$$

$$W_{swp} = m_{sw} \eta_{swp} (h_{swp,in} - h_{swp,out}) \tag{8}$$

where  $\eta_{rp}$  is the refrigerant pump’s efficiency;  $\eta_{cwp}$  and  $\eta_{swp}$  are the deep seawater and surface seawater pumps’ efficiencies; and  $h_{rp}$ ,  $h_{wwp}$ , and  $h_{cwp}$  are the enthalpies of the refrigerant pump and the surface water and deep seawater pumps. For the working fluid, R32, a pure HFC refrigerant with 0 ODP and 675 GWP, is used in this case due to its eco-friendliness and compactness [18].

### 2.1.2. Physical Theory of the OTEC System Pumps

A pump is used to pump the inlet fluid using pressure. The operation of the pump is similar to that of a compressor, but the fluid used is incompressible. The ideal power of the pump is calculated based on the standard pump equation of the following Equation (9) [19]:

$$PWR_i = \frac{(P_{out} - P_{in}) \times F}{\rho_{liq}} \tag{9}$$

where  $P_{out}$ , is the pump’s outlet pressure;  $P_{in}$  is the pump’s inlet pressure;  $F$  is the mass flow rate; and  $\rho_{liq}$  is the liquid density. The actual power of the pump is defined in the pump efficiency Equation (10):

$$\eta(\%) = \frac{PWR_i}{PWR_a} \times 100\% \tag{10}$$

The pump power applied to the pump efficiency was assumed to be the same as the motor efficiency. In Equations (9) and (10), the actual power required for pump operation can be expressed by Equation (11) below:

$$PWR_a = \frac{(P_{out} - P_{in}) \times F \times 100\%}{\rho_{liq} \times \eta(\%)} \tag{11}$$

The actual power is also equal to the enthalpy difference between the inlet and outlet fluids. If the efficiency of the pump is less than 100%, the excess energy will increase the fluid temperature at the outlet.

### 2.1.3. Material Balance

Physical changes in the OTEC during operating (e.g., flow rate, volume, density, etc.) are referred to as the ‘material balance’. Material balance is an application of the conservation of mass to the analysis of physical systems. By accounting for material entering and leaving a system, mass flows can be identified which might have been unknown. The material balance can be calculated from Equation (12):

$$\frac{d(\rho_{j0}V)}{dt} = F_i\rho_i - F_o\rho_o \tag{12}$$

where  $F_i$  is the inflow rate of water to the tank,  $\rho_i$  is the density of the supply water,  $\rho_o$  is the density of the outflow water, and  $V$  is the volume of the fluid inside the tank.

In accordance with the dynamic design of the OTEC cycle, fluid flow occurring in the system is caused by the diffusion and convection of molecules, with a dominant portion of convection flow contribution. Dynamic mass, components, and energy changes are similar to a steady-state balance, which allows the system’s output variables to change according to the time variable.

### 2.1.4. Energy Balance

The energy generated or used in the OTEC system is called the ‘energy balance’. The energy balance can be calculated using Equation (13):

$$\frac{d[(U + E_k + E_p)V]}{dt} = \left[ F_i\rho_i \left( \hat{H}_i + \frac{u_i^2}{2} + gz_i \right) - F_o\rho_o \left( \hat{H}_o + \frac{u_o^2}{2} + gz_o \right) \right] + (Q + Q_r) - [\omega + (F_oP_o - F_iP_i)] \tag{13}$$

where  $U$  is the internal energy,  $E_k$  is the kinetic energy,  $E_p$  is the potential energy: energy per unit mass,  $\omega$  is the shaft work energy driven by the system: energy per hour, and  $P_0$  is the system pressure.  $P_i$  is the pressure of the fluid inflow,  $Q$  is the heat energy passing through the boundary, and  $Q_r$  is the reactant thermal energy, but the heat of reaction is so small that it can be ignored in actual operation. Convection or conduction causes energy flux in the system. Conduction or radiation causes additional heat energy from the outer boundary layer. The energy that comes in or out of the system is specified into enthalpy ( $\hat{H}$ ), fluid velocity ( $u$ ), acceleration of gravity ( $g$ ), and distance ( $z$ ).

## 2.2. Design of the MW-Scale OTEC System

### 2.2.1. Construction of the OTEC System

The constructed turbine is applied with the theoretical operation data of the Organic Rankine Cycle (ORC) turbine, which shows an efficiency of 85% at the maximum generation capacity of 1.2 MW. In addition, flow rate and head change are measured in accordance with the RPM change in the working fluid pump made by Xylem, which is the pump company with the most advanced technology. Figure 3 shows the performance curves of the pump.

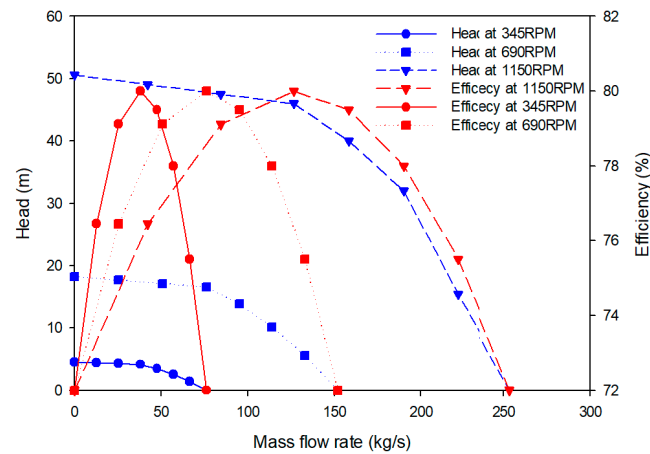


**Figure 3.** Pumping head and efficiency change in refrigerant pump flow rate.

The standard operation conditions are the temperature of 31 °C for surface seawater and 5 °C for deep seawater, the flow rates of 1236 kg/s and 1004 kg/s for surface and deep seawater, respectively, and a flow rate of 112.2 kg/s for working fluid.

Using the operating conditions shown in Table 2, a maximum output of 1010 kW, a heat capacity of 34.08 MW, and an efficiency of 2.91% were used. The rated power of the pumps was 105 kW for deep seawater, 111 kW for surface seawater, and 65.7 kW for the refrigerant. The net power of the OTEC system was 728 kW, with an efficiency of 2.13%.

**Table 2.** Specifications of the 1 MW OTEC cycle.

Design Conditions		
Surface seawater temperature	31	°C
Deep seawater temperature	5	°C
Surface seawater flow rate	1236	kg/s
Deep seawater flow rate	1004	kg/s
Refrigerant flow rate	112.2	kg/s
Surface seawater head loss	5.5	m
Deep seawater head loss	8.5	m
Surface seawater pump efficiency	75	%
Deep seawater pump efficiency	75	%
Working fluid	R32	-

### 2.2.2. Specifications of the Working Fluid Pump

The working fluid pump used in the OTEC system operates at a rotational speed up to 1150 RPM and a maximum efficiency of 80% under a mass flow rate of 126 kg/s. In addition, the pumping head shows a positive change of 46 m at the same mass flow rate and can supply a rate up to 254 kg/s. Moreover, at a mass flow rate of 126 kg/s, the head

turned out to be 46 m. However, the efficiency changes with respect to the change in the mass flow rate, with a minimum value of 72%.

Changes in the external factors of dynamic operation can lead to a reduction in the flow rate through RPM control, causing the pumping head to decrease and efficiency losses. In Section 3.2, the algorithm for preventing such a situation is applied flexibly in the dynamic simulation.

Figure 4 shows a case where two identical pumps are connected in parallel in one system. The overall performance vacancy of the system is the sum of flow rate  $Q_1$  and flow rate  $Q_2$ , and both pumps have the same head,  $H_1 = H_2$ . Since the two pumps are identical, the maximum head,  $H_{max}$ , is the same in each pump, but the maximum flow rate  $Q_{max}$  is as up to twice as large as the flow rate of one pump according to Equation (14):

$$Q_{max} = Q_1 + Q_2 = 2Q_1 = 2Q_2 \tag{14}$$

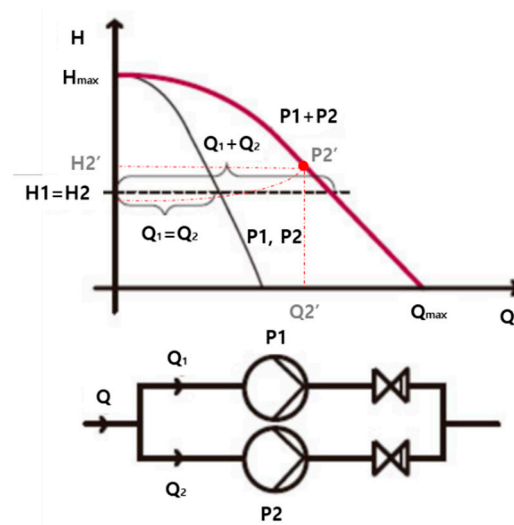


Figure 4. Performance curve when two pumps are connected in parallel.

However, in the actual operation of the pump,  $Q_2'$  is generated considering the pipe resistance  $R$ , and the head is located at  $H_2'$  according to the pipe's resistance curve. Therefore, at the time when one pump is stopped, the flow rate and head of the refrigerant pump return to  $Q_1$  and  $H_1$ . In the case of the designed OTEC, the operating head and flow rate are designed so that operation is possible within the point where net output is generated.

### 2.3. Dynamic Cycle Simulation

#### Dynamic Cycle Performance Simulation

##### (1) Pump shut down situation and expected action.

A PID (Proportional-Integral-Differential controller) is a representative type of control method most commonly used in practical applications. The PID controller basically has the form of a feedback controller. The PID controller measures an output of an object to be controlled and compares it with a normal setting condition. In this section, an analysis is performed by applying the same flow rate change that occurs when the pump is stopped. At this time, the expected results and controllable factors are analyzed.

The tested shut down situations are listed below, and the expected results with countermeasures are listed in Table 3:

- (1) Seawater pump (surface and deep seawater) stops: aging of pump, electric leakage, system blackout, damage to key components, external impact, unskilled operation technique, immersion in seawater, clogged impeller, biofouling, seawater leakage, etc.;

- (2) Refrigerant pump stops: aging of pump, electric leakage, external impact, damage to key components, refrigerant leakage, unskilled operation technique, clogged impeller, etc.

**Table 3.** Specifications of pump shut down situations.

Situation	How to Apply the Situation	Expected Result	Control Element
Sea water pump stops (surface seawater)	Rapid decrease in surface seawater flow	Separator liquid rise, turbine liquid inflow, turbine output decrease	Refrigerant pump flow control, second surface seawater pump
Sea water pump stops (deep seawater)	Rapid decrease in deep seawater flow	Separator liquid rise, turbine liquid inflow, turbine output decrease	Refrigerant pump flow control, second deep seawater pump
Refrigerant pump stops	Rapid decrease in refrigerant flow rate	Reduce turbine power	Refrigerant pump flow control, emergency stop

(2) Dynamic cycle performance with respect to pump shutdowns.

The operation monitoring time is set for 10 min, with the pump shutdown occurring 5 min after the start of the operation. The flow rate and temperature of seawater, the flow rate of the refrigerant, the heat capacity of the evaporator, the output of the turbine, and the change in the liquid level in the liquid separator were monitored. Table 4 shows the dynamic cycle parameters of the OTEC system. In general, in the case of power imbalance and malfunction, the flow rate decreases rapidly when the pump stops. However, in order to confirm the change in system performance according to the change in the flow rate, the inflow, damage by impurities in the impeller, leakage, damage to the pump discharge part, etc., were assumed. The model was designed to generate a gradual change in the flow rate per 2 minutes.

In this simulation, the reservoir tank is assumed to have a volume of 75.4 m<sup>3</sup>, and the inflow of the gas phase refrigerant is set to occur at a flow rate point of 2% in order to analyze operating conditions after hazard occurrence. In addition, the liquid refrigerant separated in the 1.5 m<sup>3</sup> class liquid separator was designed to flow into the turbine after reaching the 95% level point.

An inverter control is applied to the operating fluid pump in accordance with the change in RPM in the range of 950–1150 RPM to regulate the flow. The Honeywell PID-A model is used as the working fluid control algorithm [20].

**Table 4.** Parameter of the dynamic OTEC cycle.

Parameter	Value	Unit
Operating Condition Design		
Refrigerant pump RPM range	950~1150	RPM
Working time	600	s
First change time	290	s
Liquid volume in reservoir tank	4.54	m <sup>3</sup>
Normal operation output	980	kW
Normal warm water pump output	105	kW
Normal cold water pump output	111	kW
Normal refrigerant pump output	66	kW
Pump Shutdown Condition Design		
Decreased time in surface seawater flow	120	s
Decreased time in deep seawater flow	120	s
Decreased time in refrigerant flow	120	s

### 3. Risk Simulation and Improvement Plan Development

#### 3.1. Change in Performance with Respect to Pump Shutdowns

The change in the external factors of dynamic operation can lead to a reduction in the flow rate through RPM control, causing a decrease in the pumping head and efficiency losses. The algorithm for preventing such a situation is applied flexibly in the dynamic simulation.

##### 3.1.1. Standard Conditions

In standard conditions, the operation characteristics of the turbine and the generation efficiency are 979.2 kW and 2.92%, respectively. The refrigerant tank’s level is maintained at 28.3%, with a circulating refrigerant flow rate of 112.2 kg/s. This operation status is expected to show a decline in efficiency due to various situations of system disorder, such as low tank level and temperature changes.

##### 3.1.2. Shutdown of Surface Seawater Pump

In accordance with the shutdown of the surface seawater pump, the flow rate decreases from 1864 kg/s to 0 kg/s in 120 s after hazard outbreak. At the same time, the power generation output will decrease by about 13.9% until the seawater flow rate decreases by 40.9%. A decrease in output occurs at 8.63 kW/s for the first 22 s and will then instantaneously decrease to 0 kW. In the meantime, the level of the liquid separator increases rapidly as the evaporative heat decreases. Along with the reduction in surface seawater flow, the level of the liquid separator increases up to 100%, reached rapidly in 22 s.

As the liquid refrigerant flows into the turbine and frequent changes in the amount of heat of evaporation occur, surging and cavitation of the turbine are expected.

##### 3.1.3. Shutdown of Deep Seawater Pump

In accordance with the shutdown of the deep seawater pump, evaporative heat quantity gradually decreases until it reaches 111.4 kW/s in 110 s. Then, the rate of decline accelerates rapidly with a decrease of 905.6 kW/s for 24 s.

The deep seawater flow rate at this moment is reduced by 92.6% compared to the initial circulating flow rate. Due to the decrease in evaporative heat, the inflow of the liquid separator increases at 384 s, showing a rapid increase of 0% to 100% in a short period of time, about 18 s. Regarding the turbine’s output, the generation rate is 361.4 kW even though the flow rate decreased to 74.6 kg/s, which is a 35.8% decrease.

Unlike surface seawater pumps, deep seawater pumps show operational stability even at low flow rates of up to 10%. However, a deep seawater flow rate of less than 10% causes liquid inflow and surging in the turbines like in the surface seawater pump.

### 3.1.4. Shutdown of Refrigerant Pump

In accordance with the shutdown of the refrigerant pump, the flow rate of the refrigerant and turbine output decreases proportionally, with a rate of 1.95 kg/s and 7.83 kW/s for 58 s, respectively.

It is expected that the shutdown of the refrigerant pump will have little effect on the system due to the decreased turbine output rate. This leads to a lower risk of turbine damage caused by the inflow of liquid refrigerant and the dry operation of the pump due to the reduced flow rate of the working fluid. Figure 5 shows the changes in the OTEC system’s performance according to the shutdowns of the refrigerant pump and seawater pumps with their associated risk situations.

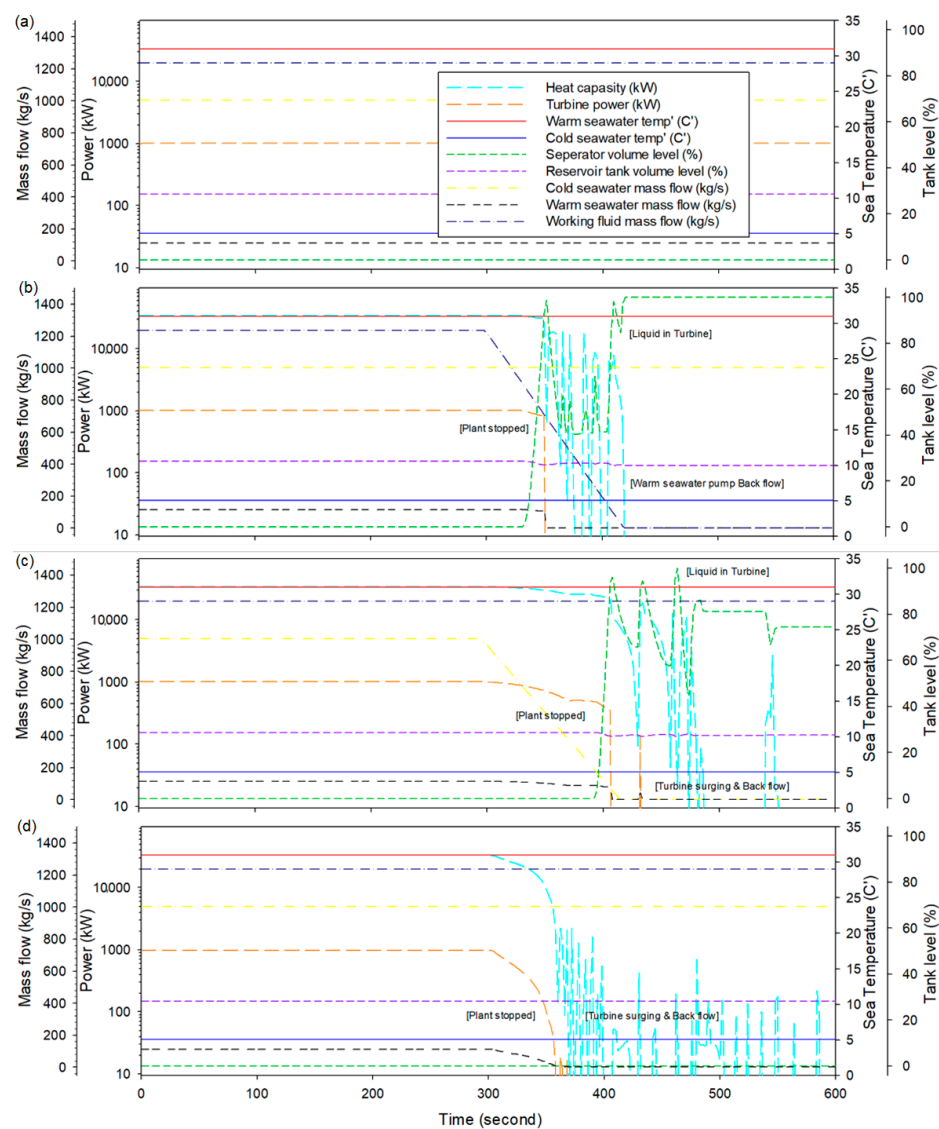


**Figure 5.** Operating condition of (a) standard conditions, (b) surface seawater pump shutdown, (c) deep seawater pump shutdown, and (d) refrigerant pump shutdown.

### 3.2. Analysis of Pump Control Solutions in MW OTEC

#### 3.2.1. Control for Surface Seawater Pump

The surface seawater pump intakes warm temperature seawater, which serves as a heat source for the refrigerant. Therefore, the shutdown of this pump directly leads to the reduction in the heat source. The prevention of this situation can be accomplished by controlling the flow rate or water lift level. In this study, a flow rate control system is adopted. Figure 6 shows the logic for starting the parallel pump operation according to the change in the pump head. When the head drops below the minimum level, the auxiliary pump is started [21]. A control method according to flow rate change was applied based on the methods of previous studies.

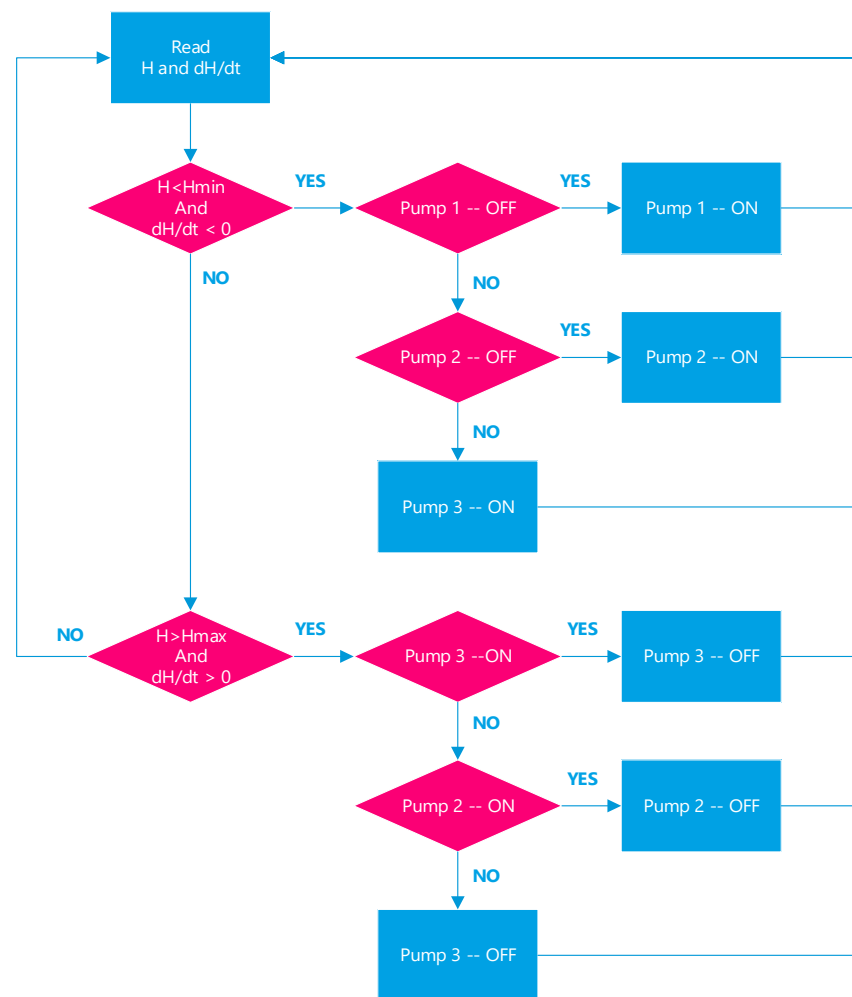


Figure 6. Control logic of auxiliary water pump (A. Malekpour).

Depending on the inflow rate of the surface seawater pump, rapid power reduction and inflow of liquid refrigerant occur in the turbine at upon reaching 59.1% of the existing flow rate. Since the system shutdown occurs at more than 50% of the total flow rate, it is expected that a system shutdown occurs when one pump in a dual pump system without an auxiliary pump stops. Therefore, the prevention of such a situation is necessary and can be achieved by adopting an auxiliary pump and parallel operation.

The ideal is to have three or more pumps, stabilizing them by operating two pumps in parallel, and using one as an auxiliary pump (used when the pump in operation stops). In addition, the parallel operation of the pumps is necessary in terms of overcoming the disadvantages of the large seawater inflow volume and high electricity usage.

For the control logic of the surface seawater pump, an auxiliary pump operates under the conditions where at least one of the two seawater pumps show a decline in flow rate. When the flow rate is unstable, even when pumps 1 and 2 are operating at the same time, an alarm signal will occur. The alarm will also activate when a seawater pump stops, when two or more pumps stop, or when the entire system has stopped. Such stand-by control is applied for system stabilization in mechanical and chemical processes [22].

### 3.2.2. Control for Deep Seawater Pump

The deep seawater pump intakes low-temperature (deep) seawater, which works as a heat sink to facilitate the OTEC plant’s operation [23]. This cooling system is similar to the seawater cooling system used in nuclear and chemical power plants.

In case the cooling system is damaged, the shutdown of the entire system is inevitable [24]. In accordance with the decrease in the deep seawater inflow rate, a rapid reduction in the output and liquid phase refrigerant inflow to the turbine occurs at the point of 8.4% performance. The solution method is similar to the method described in Table 3 (i.e., an auxiliary pump and parallel operation is necessary to ensure system safety). The logical circuit is also applicable to this section for system stabilization. Figure 7 shows the control logic for the surface and deep seawater pumps.

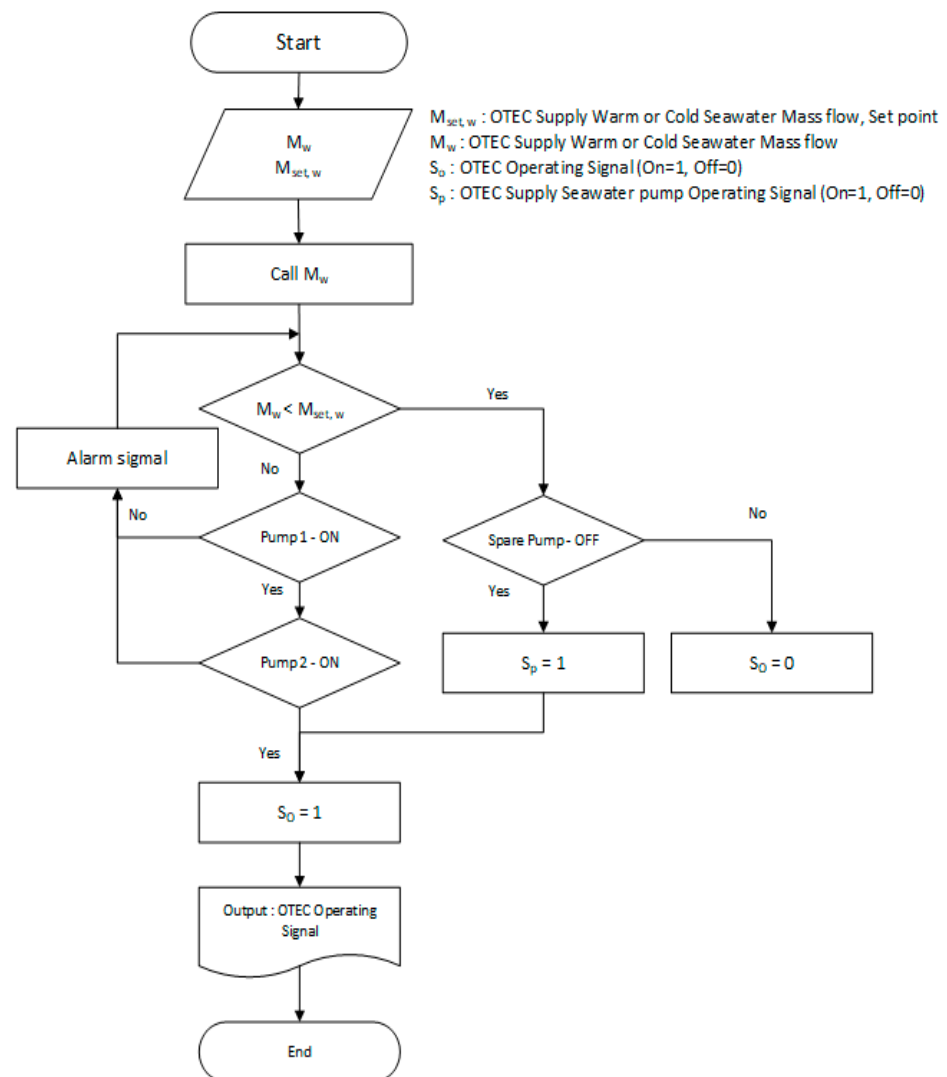


Figure 7. Control logic of surface and deep seawater pumps.

### 3.2.3. Control for Refrigerant Pump

The refrigerant circulation pump recovers heat from the surface seawater using R32, a working fluid, which then flows into the turbine as a high-temperature and high-pressure gas. The heat energy is converted into kinetic energy and then converted into a liquid refrigerant by a condenser. The reduction in turbine output and heat capacity is proportional to the decrease in the refrigerant, so there are only a few risk factors affecting the turbine and impeller, such as water hammering and the inflow of liquid refrigerant to the turbine. Moreover, by adopting a parallel operation of refrigerant pumps, risk factors are expected to be mitigated up to 50% compared to the initial system. Therefore, the improved system should be designed with two pumps. The pumps are to be operated in parallel, and when one pump stops, the other will operate independently [25].

In the improved refrigerant pump operation control model, refrigerant pumps are operated in parallel. This enables an alarm element to be selected when one of the two refrigerant pumps stops at 391.7 kW, which is an amount of power lower than the net power output, in addition to an emergency stop when both of them stop.

Figure 8 shows the control logic of the refrigerant pump. Figure 9 shows the P&ID diagram for optimal seawater and refrigerant pump control.

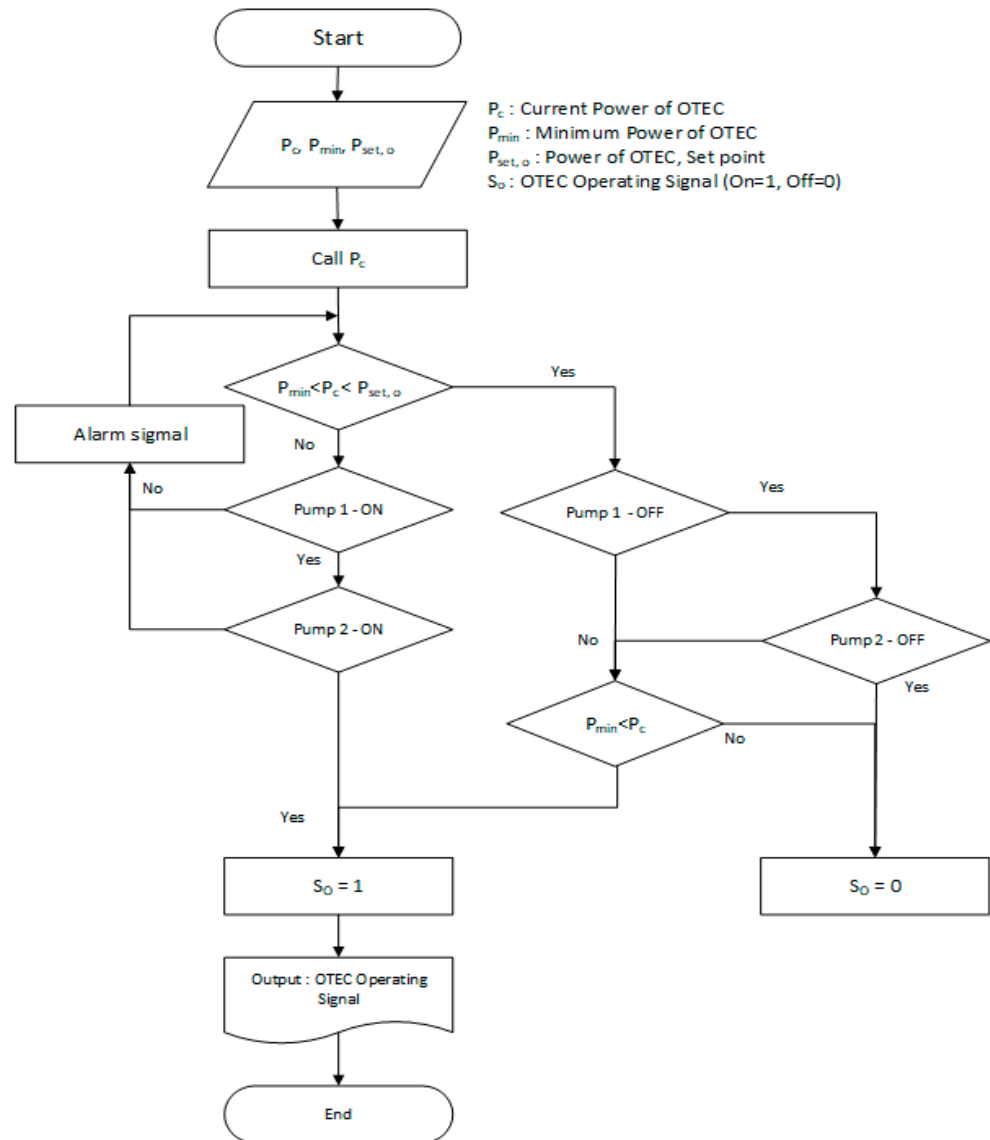


Figure 8. Control logic of the refrigerant pump.

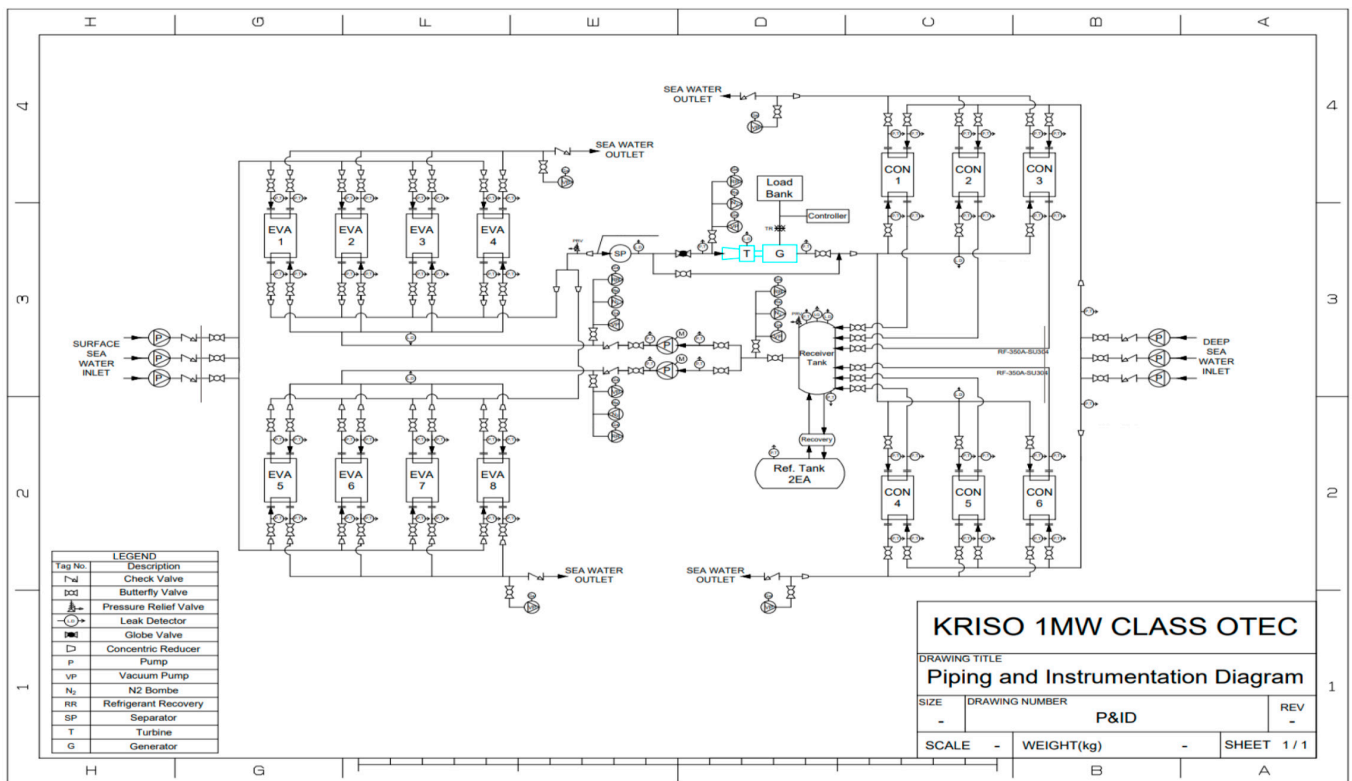


Figure 9. P&ID diagram for optimal seawater and refrigerant pump control.

#### 4. Results of OTEC Simulation with Improved Operation and Control System

##### 4.1. Simulation Results

##### 4.1.1. Shutdown of Surface Seawater Pump

As shown in Figure 10, the flow rate of surface seawater remained at 1236 kg/s despite the pump’s shutdown. In addition, in the case of individual pumps, the flow rate was 618 kg/s. The reason for this maintained flow rate is that the relative gradient of pump No. 1, which stopped operating, is equal to the same amount of water inflow caused by the auxiliary pump’s operation.

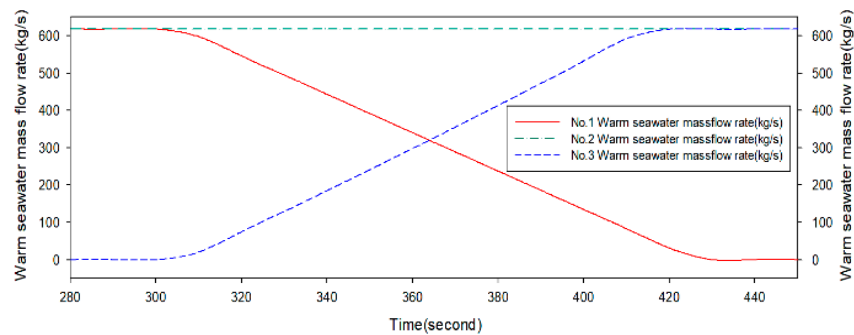


Figure 10. Flow rate gradient of surface seawater pump.

At 406 s, the maximum flow rate of the pumps is reached, with a rate of 1297 kg/s. However, if the rate of decrease in the flow rate caused by the pump shutting down is assumed to be within 60 s, the change in the flow rate of the seawater supply is expected to occur within 4.9%. On the other hand, the change in evaporation heat increased up to 22.6 kW, showing a slight increase rate of 0.069%.

In addition, when a single-pump or a double-pump system operates without using an auxiliary pump, the system cannot rehabilitate a sufficient amount of evaporation heat

when a pump shutdown occurs, which leads to the entire system shutting down. Figure 11 shows the change in the dryness of the refrigerant according to the type of pump used. Even when a double pump is used, if one pump is stopped, the liquid refrigerant still flows into the turbine after about 130 s.

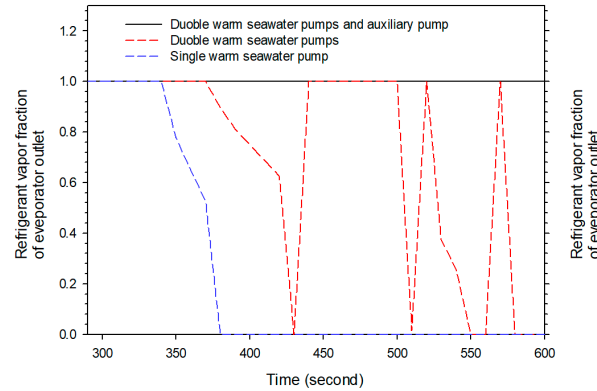


Figure 11. Vapor fraction of the refrigerant according to the type of heat pump used.

#### 4.1.2. Shutdown of Deep Seawater Pump

As shown in Figure 12, the flow rate of the deep seawater pump remained at 1004 kg/s due to the relative gradient of pumps No. 1 and No. 3. At 396 s, the pump’s flow rate reached a maximum rate of 1109 kg/s. However, if the stopped pump’s actual flow rate reduction is assumed to be within 60 s, the change in the flow rate of the deep seawater supply is assumed to be within 10.4%. On the other hand, the change in evaporation heat increases up to 39.1 kW, showing a slight increase rate of 0.12%.

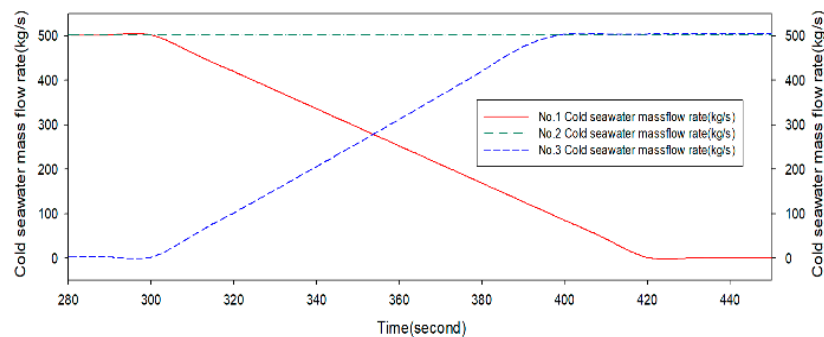


Figure 12. Flow rate gradient of deep seawater pump.

Like the surface seawater pump, the deep seawater pump does not use an auxiliary pump, and when a single-pump or a double-pump system is being used, a sufficient amount of evaporation heat cannot be secured when one pump is stopped, causing the whole system to stop. Figure 13 shows the change in the dryness of the refrigerant according to the type of pump system used. Even when a double-pump system is used, if one pump is stopped, the liquid refrigerant flows into the turbine after about 170 s.

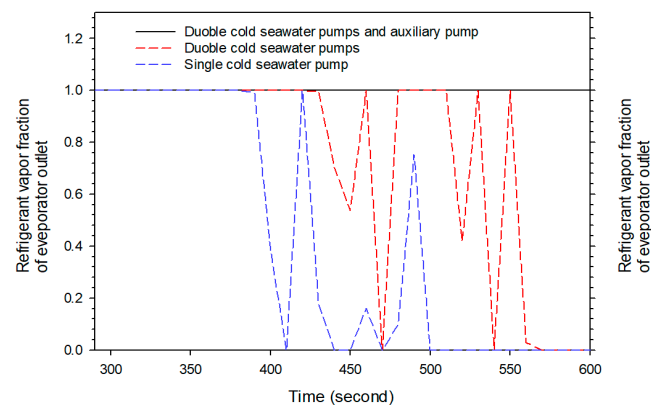


Figure 13. Vapor fraction of the refrigerant according to the type of cold pump used.

#### 4.1.3. Shutdown of Working Fluid Pump

As shown in Figure 14, in the case where a single pump shuts down while operating the pumps in parallel mode, the system is maintained by operating the auxiliary pump. Moreover, when pump No. 2 stops, the flow rate of pump No. 1 offsets the effects of the shutdown by increasing its flow rate by 53.4% from 56.2 kg/s to 86.3 kg/s. Therefore, even though pump No. 2 stops, the entire heat capacity supplied to the OTEC system is 27.1 MW, which is 79.5% of the steady-state operation (34.1 MW).

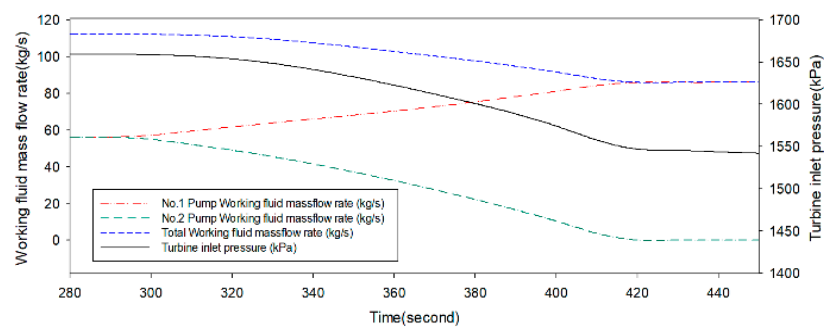


Figure 14. Inlet and outlet pressure gradient of working fluid pump.

The generation efficiency is reduced to 39.8%, which is a decline in output from 1010 kW to 595.7 kW. Nevertheless, power generation output increases to 0.213 kW/s with the increase in flow rate after decreasing to the lowest point, resulting in 617 kW of power. Even when one refrigerant pump is stopped, about 368 kW of additional power is generated compared to the OTEC’s 249 kW of electricity consumption. Considering such output, it is expected that the repair and maintenance of the pump will be possible without stopping.

This phenomenon occurs with respect to the reduction in the refrigerant supply flow rate, thus leading to the pressure loss of the turbine inlet, and the pressure difference of the inlet and outlet decreases as shown in Figure 15. Loss of turbine head and decrease in the evaporation pressure are the main causes of the flow rate of working fluid pump No. 1 increasing. For this reason, it is expected that the results of the working fluid pump No. 1’s operation showed a maximum flow rate, a 36.4 m water head condition, and a 78.9% efficiency. On the other hand, the efficiency of the turbine was reduced by 1% compared to the flow rate of a single refrigerant pump, and the outlet pressure was also reduced by 150 kPa.

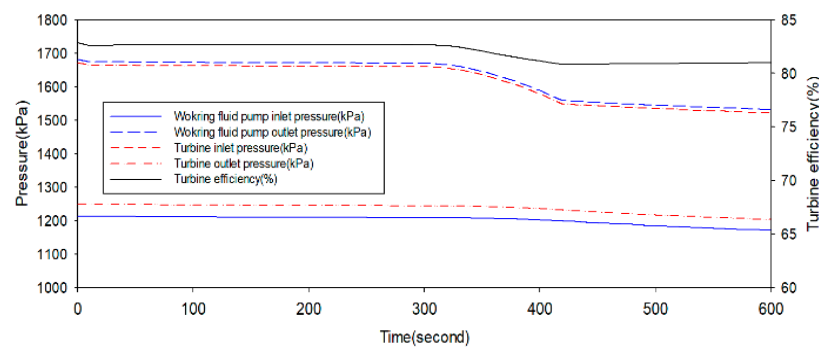


Figure 15. Flow rate gradient of working fluid pump.

4.2. Improvement Evaluation of Simulation Results

In this study, control modes were identified and presented through hazard analysis. Furthermore, the rate of system improvement is specified into low, medium, and high system improvement regarding the effect of the control module on the entire OTEC system.

The steady-state operation of the seawater pumps was able to be using parallel and auxiliary pump operation. In the case of the refrigerant pump, 40% of the total output during the operation of one of the two units was reduced, and there were no risk factors, such as the inflow of liquid refrigerant into the turbine and water hammer, so no extra pump was needed. Table 5 shows the performance results of the improved OTEC system.

Table 5. Performance results of improved OTEC.

Situation	Effects on System	Control Module	Achievements	Improvement
Surface seawater pump shutdown	-Liquid inflow to turbine -System output decrease -System shutdown	Installation of 3 pumps (2 in parallel operation, 1 spare, and alarm when pump shuts down)	-Hazard solved	High
Deep seawater pump shutdown				High
Refrigerant pump shutdown	-System shutdown -System output decrease	Parallel operation of 2 pumps (alarm when pump shuts down)	-Prevention of system shutdown	Medium

5. Conclusions

An analysis of hazard factors in an OTEC system has been carried out in this study for the establishment of an automated control system to prevent system impacts. System impacts have been analyzed via dynamic simulation, and the design of a control logic followed in order to prevent the identified impacts. As a result, an optimized P&ID control manual has been established. The following conclusions are drawn from the dynamic simulation:

(1) The suspension of the surface and deep seawater pump decreases the amount of evaporative heat and condensation heat, respectively, causing an increase in system pressure. In addition, if the degrees of the superheating and vapor fractions cannot be secured, the system is stopped along with the refrigerant flowing into the turbine. In order to control this situation, on/off control, auxiliary pump preparation, and parallel operation of the pumps have been established. This prevents the shutdown of the entire system when one pump shuts down, and the operation of the auxiliary pump operation can restore the operation to a normal range.

(2) Compared to other hazards, the effects of a refrigerant pump shutdown caused less damage to the system, such as liquid or water inflow into the turbine, water hammering, dry operation of the refrigerant pump, etc. However, by operating the refrigerant pump in parallel, the power generation system was prevented from being stopped, and it was

confirmed that the efficiency of the system was reduced by 40% compared to normal operation.

(3) Control of the number of pumps is selected according to this approach's effect on the system upon stopping one of the pumps. It is essential to apply an auxiliary pump within the range where superheating and dryness can be secured. Adequate pump operation design in OTEC can solve various pump-related risk factors such as power cut-off and operation errors that occur during operation as well as pump overdesign and volume increases.

The control modules of the OTEC system derived in this study are proposed for stabilizing the operation of power generation facilities and will be utilized to establish an optimal control system for demonstration plants.

**Author Contributions:** Conceptualization, S.L. and H.K.; methodology, S.L.; software, S.L.; validation, S.L. and J.Y.; formal analysis, J.Y.; investigation, H.L.; resources, S.L.; data curation, S.L.; writing—original draft preparation, S.L.; writing—review and editing, J.Y.; visualization, S.L.; supervision, S.L.; project administration, H.L.; funding acquisition, H.L. All authors have read and agreed to the published version of the manuscript.

**Funding:** This research was funded by The Ministry of Oceans and Fisheries, Korea, grant number (PMS5380).

**Informed Consent Statement:** [https://www.researchgate.net/publication/263965424\\_Improvement\\_of\\_the\\_Yazd\\_Water\\_Conveyance\\_Control\\_System\\_by\\_GA\\_Optimization](https://www.researchgate.net/publication/263965424_Improvement_of_the_Yazd_Water_Conveyance_Control_System_by_GA_Optimization), accessed on 4 December 2022.

**Acknowledgments:** This research was financially supported by the grant from the National R&D Project of "Demonstration of power generation system and RCI technology using ship waste heat" funded by the Ministry of Oceans and Fisheries, Korea (PMS5380).

**Conflicts of Interest:** The authors declare no conflict of interest.

## References

1. REN21. *Renewables 2019 Global Status Report*; REN21 Secretariat: Paris, France, 2019.
2. Energy Information Administration. *International Energy Outlook 2016*; EIA: Washington, DC, USA, 2016.
3. Vega, L.A. Ocean Thermal Energy Conversion. In *Encyclopedia of Sustainability Science and Technology*; Meyers, R.A., Ed.; Springer: New York, NY, USA, 2012.
4. Kim, A.S.; Kim, H.J.; Lee, H.S.; Cha, S. Dual-use open cycle ocean thermal energy conversion using multiple condensers for adjustable power generation and seawater desalination. *Renew. Energy* **2016**, *85*, 344–358. [[CrossRef](#)]
5. Lee, H.S.; Cha, S.W.; Jung, Y.G.; Choi, B.S.; Kim, H.J. Design and experiment of the 20 kW OTEC plant. In Proceedings of the KAOSTS Spring Conference, Busan, Republic of Korea, 22 May 2014; pp. 2448–2452.
6. Lim, S.T.; Kim, H.J.; Lee, H.S. Dynamic simulation of performance change of MW-class OTEC according to seawater flow rate. *J. Korean Soc. Power Syst. Eng.* **2019**, *23*, 48–56. (In Korean) [[CrossRef](#)]
7. Kwon, Y.J.; Jung, D.H.; Kim, H.J. Design of riser in 1MW OTEC system mounted on floating barge. *J. Korean Soc. Mar. Environ. Energy* **2015**, *18*, 22–28. (In Korean) [[CrossRef](#)]
8. Seo, J.B.; Moon, J.H.; Lee, H.S.; Kim, H.J. Performance evaluation and modification plan of the 1 MW OTEC turbine. In Proceedings of the Korean Science for Marine Environment & Energy Fall Conference, Busan, Republic of Korea, 8 November 2019; pp. 147–148.
9. Kim, H.-J.; Lee, H.-S.; Lim, S.-T.; Petterson, M. The Suitability of the Pacific Islands for Harnessing Ocean Thermal Energy and the Feasibility of OTEC Plants for Onshore or Offshore Processing. *Geosciences* **2021**, *11*, 407. [[CrossRef](#)]
10. Matsuda, Y.; Goto, S.; Sugi, T.; Morisaki, T.; Yasunaga, T.; Ikegami, Y. Control of OTEC Plant Using Double-stage Rankine Cycle Considering Warm Seawater Temperature Varia. *IFAC PapersOnLine* **2017**, *50*, 135–140. [[CrossRef](#)]
11. Nakamura, M.; Egashira, N.; Uehara, H. Digital Control of Working Fluid Flow Rate for an OTEC Plant. *J. Sol. Energy Eng.* **1986**, *108*, 111–116. [[CrossRef](#)]
12. Baybutt, P. On the completeness of scenario identification in process hazard analysis (PHA). *J. Loss Prev. Process Ind.* **2018**, *55*, 492–499. [[CrossRef](#)]
13. Wang, Z.; Secnik, E.; Naterer, G.F. Hazard analysis and safety assurance for the integration of nuclear reactors and thermochemical hydrogen plants. *Process Saf. Environ. Prot.* **2015**, *96*, 82–97. [[CrossRef](#)]
14. Lee, J.; Shigrekar, A.; Borrelli, R.A. Application of hazard and operability analysis for safeguardability of a pyroprocessing facility. *Nucl. Eng. Des.* **2019**, *348*, 131–145. [[CrossRef](#)]
15. Malppan, P.J.; Sumam, K.S. Pipe Burst Risk Assessment Using Transient Analysis in Surge 2000. *Aquat. Procedia* **2015**, *4*, 747–754. [[CrossRef](#)]

16. Lim, S.T.; Lee, H.S.; Moon, J.H.; Kim, H.J. Simulation Data of Regional Economic Analysis of OTEC for Applicable Area. *Processes* **2020**, *8*, 1107. [[CrossRef](#)]
17. Hendrawan, A. Calculation of Power Pumps on OTEC Power Plant Ocean (Ocean Thermal Energy Conversion). In Proceedings of the 1st International Conference on Science, Applied Science, Teaching and Education 2019, Kupang, Indonesia, 14–15 May 2019.
18. Yoon, J.-I.; Ye, B.-H.; Heo, J.-H.; Kim, H.-J.; Lee, H.-S.; Son, C.-H. Performance analysis of 20 kW OTEC power cycle using various working fluids. *J. Korean Soc. Mar. Eng.* **2013**, *37*, 836–842.
19. Song, Y.-U. A Study on the Ship's Thermal Efficiency Improvement by the ORC Power Generation System by Temperature Difference Between. Ph.D. Thesis, KMOU, Busan, Republic of Korea, 2012. Available online: [Repository.kmou.ac.kr/handle/2014.oak/9430](https://repository.kmou.ac.kr/handle/2014.oak/9430) (accessed on 13 January 2021).
20. Honeywell. *A Process Control Primer*; Honeywell: Charlotte, NC, USA, 2000.
21. Malekpour, A.; Karney, B.; Adams, B. Improvement of the Yazd Water Conveyance Control System by GA Optimization. In Proceedings of the 2nd IASTED International Conference on Water Resources Management, Honolulu, HI, USA, 20–22 August 2007.
22. Raje, D.V.; Olaniya, R.S.; Wakhare, P.D.; Deshpande, A.W. Availability assessment of a two-unit stand-by pumping system. *Reliab. Eng. Syst. Saf.* **2000**, *68*, 269–274. [[CrossRef](#)]
23. Lim, S.T.; Lee, H.S.; Kim, H.J. Dynamic Simulation of System Performance Change by PID Automatic Control of Ocean Thermal Energy Conversion. *J. Mar. Sci. Eng.* **2020**, *8*, 59. [[CrossRef](#)]
24. Song, J.; Kim, T. Severe accident issues raised by the Fukushima accident and improvements suggested. *Nucl. Eng. Technol.* **2014**, *46*, 207–216. [[CrossRef](#)]
25. Viholainen, J.; Tamminen, J.; Ahonen, T.; Ahola, J.; Vakkilainen, E.; Soukka, R. Energy-efficient control strategy for variable speed-driven parallel pumping systems. *Energy Effic.* **2013**, *6*, 495–509. [[CrossRef](#)]

**Disclaimer/Publisher's Note:** The statements, opinions and data contained in all publications are solely those of the individual author(s) and contributor(s) and not of MDPI and/or the editor(s). MDPI and/or the editor(s) disclaim responsibility for any injury to people or property resulting from any ideas, methods, instructions or products referred to in the content.